

Output-Feedback System Level Synthesis via Dynamic Programming

Lauren E. Conger and Shih-Hao Tseng

Abstract—System Level Synthesis (SLS) allows us to construct internally stabilizing controllers for large-scale systems. However, solving large-scale SLS problems is computationally expensive and the state-of-the-art methods consider only state feedback; output feedback poses additional challenges because the constraints are no longer uniquely row or column separable.

We exploit the structure of the output-feedback SLS problem by vectorizing the multi-sided matrix multiplications in the SLS optimization constraints, which allows us to reformulate it as a discrete-time control problem and solve using two stages of dynamic programming (DP). Additionally, we derive an approximation algorithm that offers a faster runtime by partially enforcing the constraints, and show that this algorithm offers the same results. DP solves SLS up to 7 times faster, with an additional 42% to 68% improvement using the approximation algorithm, than a convex program solver, and scales with large state dimensions and finite impulse response horizon.

I. INTRODUCTION

In classical control theory, transfer functions and controllers are constructed to minimize a variety of cost functions, primarily functions of the state and input [1] [2]. These celebrated techniques have been proven useful for state-feedback small-scale systems. However, in modern applications of linear control, especially for large-scale systems, the full state of a system is often unknown or too expensive to acquire within a reasonable amount of time. As a result, we rely on partial observations of the state to control the system in an output-feedback fashion. Not only does such a proxied information structure make output-feedback control difficult, but it also hinders one in incorporating additional system level constraints. To address these challenges, system level synthesis (SLS) [3], [4] derives its system level parameterization of output-feedback controllers as a convex optimization problem that maintains system-level constraint enforcement. This formulation can be used to solve the linear-quadratic Gaussian problem and optimization under the \mathcal{H}_2 norm as shown in [3]. With SLS, we can solve these traditional control problems with added system-level constraints, which is not possible with the Youla or Input-Output parameterizations [5] [6] [7].

Although convex optimization problems are in general tractable, it is still slow to solve the SLS problems for output-feedback settings. Existing work proposes to accelerate the SLS computation by exploiting the structure of underlying systems, and an early work [8] has established that an SLS problem can be solved by ADMM in theory if the problem is partially separable – for both the constraints and

the objective. In practice, most work primarily focuses on state-feedback settings [9]–[12] since the state-feedback SLS constraints are column-wise separable and we only need to ensure the objective is also column-wise separable. Output-feedback SLS is much more complicated as its constraints consist of both column-wise and row-wise separable parts, which require the objective to be both column-wise and row-wise separable for ADMM to work. As a consequence, we end up relying on the solver to deal with general non-separable output-feedback problems.

Some recent work provides an alternative approach to the SLS computation. [13] shows that a state-feedback SLS problem can be reformulated as a discrete-time control problem, which admits efficient computation via dynamic programming (DP). This approach could potentially be applied to output-feedback SLS as long as we could address the following discrepancy between the state-feedback and output-feedback SLS. First, the state-feedback SLS system response comprises only two transfer matrices, which are then conveniently set as the state and the control in [13], while the output-feedback version has four matrices to handle. Also, the system dynamics matrices are multiplied at the left in state-feedback constraints, while the output-feedback formulation have both left and right matrix multiplications in its constraints. Further, we have only one initial condition in the state-feedback SLS while the initial condition has a much more complicated structure in the output-feedback setting.

A. Contributions and Organization

We address the aforementioned challenges and extend the approach in [13] to derive a DP algorithm for output-feedback SLS by reformulating it as a discrete-time control problem. By our choice of the corresponding state and control variables, the control problem consists of a new transition constraint and initial condition compared to the state-feedback scenario. By vectorizing the multi-sided matrix multiplications, we can solve the control problem by a two-stage DP procedure. We develop the full DP and an approximation algorithm by skipping the constraint enforcement up to some *allowance*. Explicitly, we derive the algorithm for \mathcal{H}_2 and quadratic objectives. By comparing the computing time with the CVX-based solver [14], we show that DP perform up to 7 times faster. Also, the approximation algorithm can further shorten the computing time by 42% to 68% with mild accuracy degradation.

The paper is organized as follows. We begin with brief introductions of output-feedback SLS and DP in Section II. Then, we present our DP algorithms to solve and approximate output-feedback SLS in Section III. In Section IV, the

\mathcal{H}_2 and quadratic costs are explicitly derived, and we numerically evaluate our algorithms in Section V. We conclude the paper in Section VI.

B. Notation

Let $z^{-1}\mathcal{RH}_\infty$ and \mathcal{RH}_∞ denote the set of strictly proper and stable proper transfer matrices, respectively, all defined according to the underlying setting, continuous or discrete. Lower- and upper-case letters (such as x and A) denote vectors and matrices respectively, while bold lower- and upper-case characters and symbols (such as \mathbf{u} and \mathbf{R}) are reserved for signals and transfer matrices. I and 0 are the identity matrix and all-zero matrix/vector (with dimensions defined according to the context). We denote by A^+ the pseudo inverse (Moore-Penrose inverse) of A and normalize (A) the matrix containing all normalized non-zero rows in A . Let \vec{A} be the vectorized matrix A , which stacks the columns of A , and let \overleftarrow{x} be the inverse operation such that $x = \vec{\overleftarrow{A}}$ is equivalent to $A = \overleftarrow{x}$. The null space of a matrix Ψ is written as $\text{null}(\Psi) = \{v : \Psi v = 0\}$, where 0 is an all-zero vector. We denote by $\text{basis}(\mathcal{S})$ a matrix where its columns form a basis that spans the linear (sub)space \mathcal{S} .

II. PRELIMINARIES

A. Output-Feedback System Level Synthesis (SLS)

System level synthesis (SLS) allows us to design a system's closed-loop response by solving a convex optimization problem [3], [4]. For an output-feedback system evolving according to the following dynamics

$$\begin{aligned} x[t+1] &= Ax[t] + Bu[t] + d_x[t] \\ y[t] &= Cx[t] + Du[t] + d_y[t] \end{aligned}$$

where $x[t]$ is the state, $u[t]$ the control, $y[t]$ the output (measurement), and $d_x[t]/d_y[t]$ the disturbances at time t , the closed-loop system is parameterized by

$$\begin{bmatrix} \mathbf{x} \\ \mathbf{u} \end{bmatrix} = \begin{bmatrix} \Phi_{xx} & \Phi_{xy} \\ \Phi_{ux} & \Phi_{uy} \end{bmatrix} \begin{bmatrix} \mathbf{d}_x \\ \mathbf{d}_y \end{bmatrix}.$$

SLS synthesizes an internally stabilizing controller \mathbf{K} in the frequency domain by solving the convex optimization

$$\begin{aligned} \min \quad & g(\Phi_{xx}, \Phi_{xy}, \Phi_{ux}, \Phi_{uy}) \\ \text{s.t.} \quad & [zI - A \quad -B] \begin{bmatrix} \Phi_{xx} & \Phi_{xy} \\ \Phi_{ux} & \Phi_{uy} \end{bmatrix} = [I \quad 0], \\ & \begin{bmatrix} \Phi_{xx} & \Phi_{xy} \\ \Phi_{ux} & \Phi_{uy} \end{bmatrix} \begin{bmatrix} zI - A \\ -C \end{bmatrix} = \begin{bmatrix} I \\ 0 \end{bmatrix}, \\ & \Phi_{xx}, \Phi_{xy}, \Phi_{ux} \in z^{-1}\mathcal{RH}_\infty, \Phi_{uy} \in \mathcal{RH}_\infty \\ & \begin{bmatrix} \Phi_{xx} & \Phi_{xy} \\ \Phi_{ux} & \Phi_{uy} \end{bmatrix} \in \mathcal{S}, \end{aligned} \quad (1a)$$

where g is the objective and \mathcal{S} the set of system level constraints. We call $\{\Phi_{xx}, \Phi_{ux}, \Phi_{xy}, \Phi_{uy}\}$ the system response, and a solution to (1) leads to the desired controller [15, Corollary 5]

$$\mathbf{K} = \mathbf{K}_0 (I + D\mathbf{K}_0)^{-1}$$

where $\mathbf{K}_0 = \Phi_{uy} - \Phi_{ux}\Phi_{xx}^{-1}\Phi_{xy}$. The control then follows from $\mathbf{u} = \mathbf{K}\mathbf{y}$ where \mathbf{u} and \mathbf{y} are the frequency domain signals of the control u and output y .

In this paper, we consider finite impulse response (FIR) solutions with horizon T , i.e.,

$$\begin{aligned} \Phi_{xx} &= \sum_{\tau=1}^T z^{-\tau} \Phi_{xx}[\tau], & \Phi_{xy} &= \sum_{\tau=1}^T z^{-\tau} \Phi_{xy}[\tau], \\ \Phi_{ux} &= \sum_{\tau=1}^T z^{-\tau} \Phi_{ux}[\tau], & \Phi_{uy} &= \sum_{\tau=0}^T z^{-\tau} \Phi_{uy}[\tau], \end{aligned}$$

where $\Phi_{\bullet}[\tau]$ are the corresponding spectral components. Notice that the summation limit is different for Φ_{uy} due to (1a). Further, we assume that the objective g is a finite sum of per-step costs:

$$\begin{aligned} g(\Phi_{xx}, \Phi_{xy}, \Phi_{ux}, \Phi_{uy}) \\ = \sum_{\tau=0}^T g_\tau(\Phi_{xx}[\tau], \Phi_{xy}[\tau], \Phi_{ux}[\tau], \Phi_{uy}[\tau]). \end{aligned}$$

B. Dynamic Programming (DP)

Dynamic programming (DP) breaks down a cost-optimization problem into a series of subproblems recursively correlated to each other. The optimal solution to the original problem can then be obtained by iteratively solving the subproblems. Such a breakdown is possible especially when the overall cost h is the sum of per-step costs h_τ , e.g.,

$$h(\mathbf{x}, \mathbf{u}) = \sum_{\tau=0}^T h_\tau(x[\tau], u[\tau]).$$

Letting $x[\tau+1] = f(x[\tau], u[\tau])$, DP then derives the cost-to-go functions $V_\tau(x[\tau])$ from the Bellman equation:

$$V_\tau(x[\tau]) = \min_{\hat{u} \in \mathcal{A}_u[\tau]} h_\tau(x[\tau], \hat{u}) + V_{\tau+1}(f(x[\tau], \hat{u}))$$

where $\mathcal{A}_u[\tau]$ is the set of admissible $u[\tau]$ and $V_{T+1}(x[\tau]) = 0$. As such, given the initial condition $x[0]$, the optimal cost of the original problem is $V_0(x[0])$, and the optimal $u[\tau]$ is the one achieving the minimum of the cost-to-go function $V_\tau(x[\tau])$, i.e.,

$$\begin{aligned} u[\tau] &= \underset{\hat{u} \in \mathcal{A}_u[\tau]}{\text{argmin}} h_\tau(x[\tau], \hat{u}) + V_{\tau+1}(f(x[\tau], \hat{u})) \\ &= K_\tau(x[\tau]). \end{aligned} \quad (2)$$

Meanwhile, we can also use the above $u[\tau]$ to express $V_\tau(x[\tau])$ as

$$V_\tau(x[\tau]) = h_\tau(x[\tau], u[\tau]) + V_{\tau+1}(f(x[\tau], u[\tau])). \quad (3)$$

C. Useful Lemmas

Below are some useful lemmas that we will use in our derivations later. We omit the proofs as they are all trivial.

Lemma 1 (Lemma 1 in [13]). *Given a matrix Ψ , $\text{null}(\Psi)$ is a subspace and there exists some matrix $\Xi = \text{basis}(\text{null}(\Psi))$.*

Lemma 2 (Lemma 2 in [13]). *The intersection of $\text{null}(\Psi_a)$ and $\text{null}(\Psi_b)$ is $\text{null}\left(\begin{bmatrix} \Psi_a \\ \Psi_b \end{bmatrix}\right)$.*

Lemma 3. *Given matrices Γ and Z , we have*

$$\Gamma^+ Z = \underset{M}{\operatorname{argmin}} \|\Gamma M - Z\|.$$

Lemma 4. *Letting Ψ be a matrix with at least one non-zero row, we have $\text{null}(\Psi) = \text{null}(\text{normalize}(\Psi))$.*

III. DP ALGORITHMS FOR OUTPUT-FEEDBACK SLS

In the following, we provide our DP algorithms to solve the output-feedback SLS (1) with the set of system level constraints (\mathcal{S}). We first reformulate the SLS problem as a control problem, which then allows us to apply DP to derive explicit and approximation solutions efficiently.

A. Control Problem Reformulation

We can reformulate the SLS optimization (1) as a control problem by treating the system response $\{\Phi_{xx}, \Phi_{ux}, \Phi_{xy}, \Phi_{uy}\}$ as the state \mathbf{x} and the input \mathbf{u} of a linear system. Accordingly, we can rewrite the cost function $g(\Phi_{xx}, \Phi_{xy}, \Phi_{ux}, \Phi_{uy})$ in terms of the state and input as $h(\mathbf{x}, \mathbf{u})$, resulting in a state-feedback control problem. As such, we can apply DP to solve the control problem, which equivalently solves the original SLS optimization. Below, we describe the reformulation in detail.

Let \vec{A} be the stacked column vectors of a matrix A , we slightly abuse the notation to overwrite/define

$$x[\tau] = \begin{bmatrix} x_{xx}[\tau] \\ x_{xy}[\tau] \\ x_{ux}[\tau] \end{bmatrix} = \begin{bmatrix} \vec{\Phi_{xx}[\tau]} \\ \vec{\Phi_{xy}[\tau]} \\ \vec{\Phi_{ux}[\tau]} \end{bmatrix}, \quad u[\tau] = \vec{\Phi_{uy}[\tau]},$$

and define the per-step cost h_τ to be

$$h_\tau(x[\tau], u[\tau]) = g_\tau(\Phi_{xx}[\tau], \Phi_{xy}[\tau], \Phi_{ux}[\tau], \Phi_{uy}[\tau]).$$

Since we consider only FIR system response with horizon T , the constraint set in (1) can be written as

$$\begin{aligned} \Phi_{xx}[\tau+1] &= \Phi_{xx}[\tau]A + \Phi_{xy}[\tau]C \\ \Phi_{xy}[\tau+1] &= A\Phi_{xy}[\tau] + B\Phi_{uy}[\tau] \\ \Phi_{ux}[\tau+1] &= \Phi_{ux}[\tau]A + \Phi_{uy}[\tau]C \end{aligned}$$

for all $\tau = 1, \dots, T-1$,

$$A\Phi_{xx}[\tau] + B\Phi_{ux}[\tau] = \Phi_{xx}[\tau]A + \Phi_{xy}[\tau]C$$

for all $\tau = 1, \dots, T$, and

$$\begin{aligned} \Phi_{xx}[0] &= 0, & \Phi_{xy}[0] &= 0, & \Phi_{ux}[0] &= 0, \\ \Phi_{xx}[1] &= I, & \Phi_{xy}[1] &= B\Phi_{uy}[0], & \Phi_{ux}[1] &= \Phi_{uy}[0]C \end{aligned}$$

We can rewrite the above equations in terms of $x[\tau]$ and $u[\tau]$. Let \mathcal{S}_x and \mathcal{S}_u be sets such that if $\Phi \in \mathcal{S}$ then $\mathbf{x} \in \mathcal{S}_x$

and $\mathbf{u} \in \mathcal{S}_u$. This reformulates (1) as

$$\min \sum_{\tau=0}^T h_\tau(x[\tau], u[\tau]) \quad (4)$$

$$\text{s.t. } x[\tau+1] = \tilde{A}x[\tau] + \tilde{B}u[\tau] \quad \forall \tau = 1, \dots, T-1 \quad (4a)$$

$$\tilde{A}_{eq}x[\tau] = 0 \quad \forall \tau = 1, \dots, T \quad (4b)$$

$$x[0] = 0, x[1] = \begin{bmatrix} \vec{I} \\ \tilde{B}_0 u[0] \end{bmatrix} \quad (4c)$$

$$\tilde{A}x[T] + \tilde{B}u[T] = 0 \quad (4d)$$

$$x[\tau] \in \mathcal{S}_x[\tau], \quad u[\tau] \in \mathcal{S}_u[\tau] \quad (4e)$$

where \tilde{A} , \tilde{B} , and \tilde{A}_{eq} are derived according to the SLS conditions.

Notice that given $x[\tau]$ as the state and $u[\tau]$ as the control at time τ , (4) can be seen as a discrete-time state-feedback control problem with state dynamics (4a), transition constraint (4b), initial condition (4c), boundary condition (4d), and system-level constraints (4e).

B. Explicit Solution by Dynamic Programming

Since (4) is a state-feedback problem, we can adopt a similar procedure as in [13] to solve it. Specifically, we need to

- *backward recursion:* recursively compute $V_\tau(x[\tau])$ backwards in τ based on (4a);
- *transition constraint and boundary condition:* enforce (4b), (4d), and (4e) throughout the derivation.
- *initial condition:* enforce (4c).

In this paper, we show how to derive the DP procedure for unconstrained SLS, i.e., (4) without system-level constraints (4e), and we could easily extend our results here to handle entrywise linear (4e) using similar techniques as in [13, Section II C].

We examine these three aspects below.

Backward recursion: For the backward recursion, we can set

$$f(x[\tau], u[\tau]) = \tilde{A}x[\tau] + \tilde{B}u[\tau]$$

and apply the procedure in Section II-B to derive $V_\tau(x[\tau])$ and $u[\tau]$.

Transition constraint, system constraint, and boundary condition: We enforce (4b) and (4d) during the recursion, which requires maintaining the admissible input set $\mathcal{A}_u[\tau]$ as shown in [13]. A result in [13] iteratively shows that $x[\tau]$ lies in the null space of some matrix $\Psi_x[\tau]$ and derives $\mathcal{A}_u[\tau]$ accordingly. However, we cannot directly adopt the results from [13] to derive $\mathcal{A}_u[\tau]$ as we have the new condition (4b) to meet. Fortunately, [13] combines its Corollary 1 and equation (11) to deal with additional conditions for $x[\tau]$ (the entrywise linear condition), and we can borrow such a concept to derive the following theorem for our output-feedback scenario to handle the new condition (4b).

Theorem 1. Suppose $x[\tau + 1] \in \text{null}(\Psi_x[\tau + 1])$ for some given matrix $\Psi_x[\tau + 1]$. For $\tau \geq 1$, we have

$$\mathcal{A}_u[\tau] = \{\hat{u} : \hat{u} = H_x x[\tau] + H_\lambda \lambda\}$$

where

$$\begin{aligned}\Gamma &= [-\tilde{B} \quad \Xi_x[\tau + 1]], \\ H_x &= [I \quad 0] \Gamma^+ \tilde{A}, \\ H_\lambda &= [I \quad 0] (I - \Gamma^+ \Gamma),\end{aligned}$$

and $\Xi_x[\tau + 1] = \text{basis}(\text{null}(\Psi_x[\tau + 1]))$.

Also, $x[\tau] \in \text{null}(\Psi_x[\tau])$ where

$$\Psi_x[\tau] = \begin{bmatrix} (\Gamma \Gamma^+ - I) \tilde{A} \\ \tilde{A}_{eq} \end{bmatrix}.$$

Proof. Without condition (4b), the former part follows directly from [13, Corollary 1]. Since (4b) is equivalent to $x[\tau] \in \text{null}(\tilde{A}_{eq})$, the theorem follows from Lemma 2. \square

Using Theorem 1, we can define $\Psi_x[T + 1] = I$ and backward-recursively derive each $\mathcal{A}_u[\tau]$ and $\Psi_x[\tau]$ to enforce (4b) and (4d). Though Theorem 1 works in theory, in practice the computation of the pseudo-inverse Γ^+ can hardly be done precisely. The numerical error then affects the precision of the matrix Ψ_x , which further disturbs the resulting basis Ξ_x and causes numerical instability. Therefore, we propose the following theorem that leads to a more numerically stable derivation of H_x and H_λ .

Theorem 2. Let

$$\Gamma_A = \Psi_x[\tau + 1] \tilde{A}, \quad \Gamma_B = \Psi_x[\tau + 1] \tilde{B}.$$

H_x and H_λ in Theorem 1 can be alternatively computed by

$$\begin{aligned}H_x &= \underset{M}{\text{argmin}} \|\Gamma_B M + \Gamma_A\|, \\ H_\lambda &= \text{basis}(\text{null}(\Gamma_B)).\end{aligned}$$

Also, $x[\tau] \in \text{null}(\Psi_x[\tau])$ where

$$\Psi_x[\tau] = \text{normalize} \left(\begin{bmatrix} \Gamma_B H_x + \Gamma_A \\ \tilde{A}_{eq} \end{bmatrix} \right).$$

Proof. Since $x[\tau + 1] \in \text{null}(\Psi_x[\tau + 1])$, we have

$$\begin{aligned}\Psi_x[\tau + 1] x[\tau + 1] &= \Psi_x[\tau + 1] (\tilde{A} x[\tau] + \tilde{B} u[\tau]) \\ &= \Gamma_A x[\tau] + \Gamma_B u[\tau] = 0.\end{aligned}$$

Therefore, we know

$$\begin{aligned}\Gamma_B u[\tau] &= -\Gamma_A x[\tau] \\ \Rightarrow u[\tau] &= -\Gamma_B^+ \Gamma_A x[\tau] + (I - \Gamma_B^+ \Gamma_B) \lambda' \\ &= H_x x[\tau] + H_\lambda \lambda' .\end{aligned}$$

H_x can then be computed by Lemma 3. On the other hand, we know $\Gamma_B H_\lambda \lambda' = 0$. Therefore, $H_\lambda \lambda' \in \text{null}(\Gamma_B)$, and we can reparameterize the space by setting $H_\lambda = \text{basis}(\text{null}(\Gamma_B))$. Lastly, the solution to the above equation exists if and only if

$$(-\Gamma_B \Gamma_B^+ \Gamma_A + \Gamma_A) x[\tau] = (\Gamma_B H_x + \Gamma_A) x[\tau] = 0.$$

Therefore, $x[\tau] \in \text{null}(\Gamma_B H_x + \Gamma_A)$. Along with $x[\tau] \in \text{null}(\tilde{A}_{eq})$, we can derive $\Psi_x[\tau]$ via Lemma 2 and Lemma 4. \square

Theorem 2 provides a numerically more stable procedure to compute H_x and H_λ , and while we leave this proof for future work, our experiments indicate that

- H_x can be computed by regression, which can be done via some sophisticated algorithms;
- H_λ have a smaller dimension;
- the normalized Ψ_x is less likely to suffer resolution issues.

Initial condition: Under the state-feedback scenario in [13], we only need to set $\Phi_{xx}[1] = I$ at the end to enforce the initial condition. However, under our output-feedback setting, we have two sets of initial conditions. We need to ensure both $x[0]$ and $x[1]$ in (4c). Therefore, we partition the whole backward recursion into two phases: from T to 1 and from 1 to 0. For the former phase, we derive $\mathcal{A}_u[\tau]$ and $\Psi_x[\tau]$ recursively according to Theorem 2 until we obtain $\Psi_x[1]$. In the next phase, we derive $\mathcal{A}_u[0]$ using the following theorem.

Theorem 3. Suppose $x[1] \in \text{null}(\Psi_x[1])$ for some given matrix $\Psi_x[1]$ where $\Psi_x[1] = [\Psi_{x_1}[1] \quad \Psi_{x_2}[1]]$ such that

$$\Psi_{x_1}[1] x_{xx}[1] + \Psi_{x_2}[1] \begin{bmatrix} x_{xy}[1] \\ x_{ux}[1] \end{bmatrix} = 0.$$

We have

$$\mathcal{A}_u[0] = \{\hat{u} : \hat{u} = w + H_\lambda \lambda\}$$

where

$$\begin{aligned}\Gamma &= \Psi_{x_2}[1] \tilde{B}_0, \\ w &= \underset{M}{\text{argmin}} \left\| \Gamma + \Psi_{x_1}[1] \vec{I} \right\|, \\ H_\lambda &= \text{basis}(\text{null}(\Gamma)).\end{aligned}$$

Proof. Since $x[1] \in \text{null}(\Psi_x[1])$, we have

$$\begin{aligned}\Psi_x[1] x[1] &= 0 = \Psi_x[1] \begin{bmatrix} \vec{I} \\ \tilde{B}_0 u[0] \end{bmatrix} \\ &= \Psi_{x_1}[1] \vec{I} + \Psi_{x_2}[1] \tilde{B}_0 u[0].\end{aligned}$$

Rearrange the terms and we obtain

$$\Psi_{x_2}[1] \tilde{B}_0 u[0] = \Gamma u[0] = -\Psi_{x_1}[1] \vec{I}.$$

Therefore,

$$u[0] = -\Gamma^+ \Psi_{x_1}[1] \vec{I} + (I - \Gamma^+ \Gamma) \lambda.$$

We can then show the results following the same procedure in the proof of Theorem 2. \square

Combining both Theorem 2 and Theorem 3, we can derive admissible input sets $\mathcal{A}_u[\tau]$ for all $\tau = 0, \dots, T$. Let \vec{x} rebuild a matrix A such that $\vec{A} = x$, we present our DP output-feedback SLS in Algorithm 1.

Algorithm 1 DP for output feedback SLS

Input: Per-step costs $g_\tau(\Phi_{xx}[\tau], \Phi_{xy}[\tau], \Phi_{ux}[\tau], \Phi_{uy}[\tau])$ for all $\tau = 0, \dots, T$ and the matrices A , B , and C in (1).
Output: $\Phi_{xx}[\tau], \Phi_{xy}[\tau], \Phi_{ux}[\tau], \Phi_{uy}[\tau]$ for all $\tau = 0, \dots, T$.
1: Derive h_τ from g_τ for all $\tau = 0, \dots, T$.
2: Derive \hat{A} , \hat{B} , \hat{A}_{eq} , and \hat{B}_0 from A , B and C according to (1).
3: $\Psi_x[T+1] = I$.
4: $V_{T+1}(x[T+1]) = 0$.
5: **for** $\tau = T, \dots, 1$ **do**
6: Derive $\mathcal{A}_u[\tau]$ and $\Psi_x[\tau]$ by Theorem 2.
7: Compute $K_\tau(x[\tau])$ by (2).
8: Derive $V_\tau(x_\tau)$ by (3).
9: **end for**
10: Derive $\mathcal{A}_u[0]$ by Theorem 3.
11: Compute $u[0]$ by (2).
12: Set $\Phi_{uy}[0] = \overleftarrow{u[0]}$ and $\Phi_{xx}[0] = \Phi_{xy}[0] = \Phi_{ux}[0] = 0$.
13: Compute $x[1]$ by (4c).
14: **for** $\tau = 1, \dots, T$ **do**
15: $u[\tau] = K_\tau(x[\tau])$.
16: Set $\Phi_{xx}[\tau] = \overleftarrow{xx[\tau]}$, $\Phi_{xy}[\tau] = \overleftarrow{xy[\tau]}$, $\Phi_{ux}[\tau] = \overleftarrow{ux[\tau]}$, and $\Phi_{uy}[\tau] = \overleftarrow{u[\tau]}$.
17: $x[\tau+1] = \hat{A}x[\tau] + \hat{B}u[\tau]$.
18: **end for**

C. Approximation for Faster Computation

Though Theorem 2 has greatly improved the numerical stability and simplified computation over Theorem 1, calculating the matrices in Theorem 2 is still computationally expensive. Therefore, we explore the possibility of an approximation algorithm which trades the precision for faster computation. Inspired by the approximation to the infinite horizon SLS problem in [13], we can relax (4b) and (4d) by using

$$H_x = 0, \quad H_\lambda = I,$$

which is equivalent to an unconstrained \mathcal{A}_u , and reuse $\Psi_x[T_a]$ as $\Psi_x[1]$ for Theorem 3 where T_a is the *allowance*, that is, the number of time steps at which we use an unconstrained \mathcal{A}_u . We summarize this approximation in Algorithm 2. We observe imperically that the null space defining \mathcal{A}_u is close enough to \mathbb{R}^n that it is practically useful; we defer proof of this to future work.

IV. EXAMPLE ALGORITHMS

Now that we have defined the dynamic programming algorithms, we illustrate results for two classes of objective functions. We show algorithms for computing the optimal control under two cost functions: a \mathcal{H}_2 and a quadratic cost. Define the \mathcal{H}_2 cost to be

$$h_\tau(x[\tau], u[\tau]) = \|Fx[\tau] + Gu[\tau]\|_F^2,$$

Algorithm 2 DP Approximation for output feedback SLS

Input: Per-step costs $g_\tau(\Phi_{xx}[\tau], \Phi_{xy}[\tau], \Phi_{ux}[\tau], \Phi_{uy}[\tau])$ for all $\tau = 0, \dots, T$, the matrices A , B , and C in (1), and allowance T_a .
Output: $\Phi_{xx}[\tau], \Phi_{xy}[\tau], \Phi_{ux}[\tau], \Phi_{uy}[\tau]$ for all $\tau = 0, \dots, T$.
1: Follow line 1 to 4 in Algorithm 1.
2: **for** $\tau = T, \dots, T_a$ **do**
3: Perform line 6 to 8 in Algorithm 1.
4: **end for**
5: **for** $\tau = T_a, \dots, 1$ **do**
6: Compute $K_\tau(x[\tau])$ by (2) with unconstrained $\mathcal{A}_u[\tau]$.
7: Derive $V_\tau(x_\tau)$ by (3).
8: **end for**
9: Let $\Psi_x[1] = \Psi_x[T_a]$.
10: Perform line 10 to 18 in Algorithm 1.

where $\|\cdot\|_F$ is the Frobenius norm, and the quadratic cost to be

$$h_\tau(x[\tau], u[\tau]) = x[\tau]^\top Qx[\tau] + u[\tau]^\top Ru[\tau],$$

where Q is a positive definite matrix weighing the cost of elements of the state. Note that the \mathcal{H}_2 objective is a generalization of the quadratic objective where cross terms between x and u are permitted.

A. \mathcal{H}_2 Objective

Using the reformulated SLS constraint and optimization equations (4), we implement a dynamic programming algorithm by deriving an explicit expression for the cost-to-go function from the objective function g_τ . For $\tau > 0$, we have:

$$V_\tau(x[\tau]) = \min_{\hat{u} \in \mathcal{A}_u[\tau]} \|Fx[\tau] + G\hat{u}\|_F^2 + V_{\tau+1}(f(x[\tau], \hat{u})).$$

Using the form of U from Theorem 1 and the claim in equation 12 in [13], we know that the cost-to-go function can be parameterized by some matrix P .

$$V_\tau(x[\tau]) = \min_{\lambda} \{ \|Fx[\tau] + G_\lambda \lambda\|_F^2 + \sum_{t=\tau+1}^T \|P[t](A_x x[t] + B_\lambda \lambda)\|_F^2 \}$$

where

$$\begin{aligned} A_x &= A + BH_x, & B_\lambda &= BH_\lambda, \\ F_x &= F + GH_x, & G_\lambda &= GH_\lambda. \end{aligned}$$

After solving for the λ that minimizes the function, which then gives a controller as a function of the state, the cost-to-go is given by

$$V_\tau(x[\tau]) = \min_{\lambda} \{ \|(F + GK[\tau])x[\tau]\|_F^2 + \sum_{t=\tau+1}^T \|P[t](A + BK[t])x[t]\|_F^2 \}.$$

where

$$\begin{aligned} K[\tau] &= H_x + H_\lambda L[\tau] \\ L[\tau] &= -(G_\lambda^\top G_\lambda + B_\lambda^\top P[\tau] B_\lambda)^{-1} (G_\lambda^\top F_x + B_\lambda^\top P[\tau] A_x). \end{aligned} \quad (5)$$

[13] shows how to compute $P[\tau]$; we state the result here:

$$\begin{aligned} P[\tau - 1] &= (C + GK[\tau])^\top (C + GK[\tau]) \\ &\quad + (A + BK[\tau])^\top P[\tau] (A + BK[\tau]). \end{aligned} \quad (6)$$

The derivation changes from the state feedback scenario for $\tau = 0$. The SLS constraints that hold for the previous transitions change, so the cost-to-go is instead given as an optimization over a control input that influences Φ_{xy} , Φ_{ux} , and Φ_{uy} . Recall $P[1]$ as the matrix defining the cost-to-go at the next state, where the cost-to-go at state $x[1]$ is $V_1(x[1]) = \|P[1]x[1]\|_F^2$.

$$V_0(x[0]) = \min_{\hat{u} \in \mathcal{A}_u[0]} \left\{ \|G\hat{u}\|_F^2 + \left\| P[1] \begin{bmatrix} \vec{I} \\ \tilde{B}_0 \hat{u} \end{bmatrix} \right\|_F^2 \right\}$$

Now we must consider the form that $u[0]$ will take. We showed in Theorem 3 that $\mathcal{A}_u[0]$ consists of vectors of the form $\hat{u} = H_\lambda \lambda + w$. We can write the cost-to-go as

$$\begin{aligned} V_0(x[0]) &= \min_{\lambda} \left\{ \|G(H_\lambda \lambda + w)\|_F^2 + \left\| P[1] \begin{bmatrix} \vec{I} \\ \tilde{B}_0(H_\lambda \lambda + w) \end{bmatrix} \right\|_F^2 \right\} \end{aligned}$$

and the control parameterization as

$$\begin{aligned} u[0] &= H_\lambda \lambda^* + w, \\ \lambda^* &= \operatorname{argmin}_{\lambda} \left\{ \|G(H_\lambda \lambda + w)\|_F^2 + \left\| P[1] \begin{bmatrix} \vec{I} \\ \tilde{B}_0(H_\lambda \lambda + w) \end{bmatrix} \right\|_F^2 \right\}. \end{aligned} \quad (7)$$

The solution can be found by setting the derivative equal to zero and solving for λ^* . The steps are shown in Algorithm 3.

B. Quadratic Objective

Now we consider the algorithm under the quadratic objective. We derive an explicit cost-to-go function under this objective as

$$V_\tau(x[\tau]) = \min_{\hat{u} \in \mathcal{A}_u[\tau]} x[\tau]^\top Q x[\tau] + \hat{u}^\top R \hat{u} + V_{\tau+1}(f(x[\tau], \hat{u})).$$

Starting from $\tau = T$ and recursively computing backward, from [13] we have that $V_\tau(x[\tau])$ can be written as $x[\tau]^\top V_{(\tau)} x[\tau]$. We know the future cost at time $\tau = T$ is zero, and $u[T]$ takes the form $u[T] = H_\lambda \lambda + H_x x[T]$, so we can write the overall cost-to-go as

$$\begin{aligned} V_T(x[T]) &= \min_{\lambda} x[T]^\top Q x[T] \\ &\quad + (H_\lambda \lambda + H_x x[T])^\top R (H_\lambda \lambda + H_x x[T]). \end{aligned}$$

Algorithm 3 DP with \mathcal{H}_2 Objective

Input: Per-step costs $g_\tau(\Phi_{xx}[\tau], \Phi_{xy}[\tau], \Phi_{ux}[\tau], \Phi_{uy}[\tau])$ for all $\tau = 0, \dots, T$ and the matrices A , B , and C in (1); F and G .

Output: $\Phi_{xx}[\tau], \Phi_{xy}[\tau], \Phi_{ux}[\tau], \Phi_{uy}[\tau]$ for all $\tau = 0, \dots, T$.

- 1: Derive h_τ from g_τ for all $\tau = 0, \dots, T$.
 - 2: Derive \tilde{A} , \tilde{B} , \tilde{A}_{eq} , and \tilde{B}_0 from A , B and C according to (1).
 - 3: $\Psi_x[T+1] = I$.
 - 4: $P[T] = 0$.
 - 5: **for** $\tau = T, \dots, 1$ **do**
 - 6: Derive \mathcal{A}_u and $\text{null}(\Psi_x[\tau])$ by Theorem 2.
 - 7: Compute $K_\tau(x_\tau)$ by (5).
 - 8: Compute $P[\tau - 1]$ from $P[\tau]$ by (6).
 - 9: **end for**
 - 10: Derive $\mathcal{A}_u[0]$ by Theorem 3.
 - 11: Compute $u[0]$ by (7).
 - 12: Set $\Phi_{uy}[0] = u[0]$ and $\Phi_{xx}[0] = \Phi_{xy}[0] = \Phi_{ux}[0] = 0$.
 - 13: Compute $x[1]$ by (4c).
 - 14: Perform line 14 to 18 in Algorithm 1.
-

After solving for the value of λ that minimizes $V_T(x[T])$, and assuming that R is symmetric, we can write the cost as

$$\begin{aligned} V_T(x[T]) &= x[T]^\top V_{(T)} x[T] \\ \text{where } V_{(T)} &= Q + \tilde{Q} \\ \tilde{Q} &= \tilde{Q}^\top R \tilde{Q} \\ \tilde{Q} &= I - H_\lambda (H_\lambda^\top R H_\lambda)^{-1} H_x. \end{aligned}$$

Each $V_\tau(x[\tau])$ can also be written in this quadratic form. Pugging in the form of $u[\tau]$ and the quadratic form of the future cost-to-go function, we set the derivative equal to zero and solve for the λ which minimizes $V_\tau(x[\tau])$, resulting in the following definitions for $V_\tau(x[\tau])$ and $K[\tau]$:

$$\begin{aligned} V(x[\tau]) &= x[\tau]^\top V_{(\tau)} x[\tau] \quad \text{where} \\ V_{(\tau)} &= Q + K[\tau]^\top R K[\tau] + \\ &\quad (\tilde{A} + \tilde{B}K[\tau])^\top V_{(\tau+1)} (\tilde{A} + \tilde{B}K[\tau]) \end{aligned} \quad (8)$$

and

$$\begin{aligned} K[\tau] &= H_x - H_\lambda L_d^{-1} L_n \quad \text{where} \\ L_d &= H_\lambda^\top R H_\lambda + (\tilde{B}H_\lambda)^\top V_{(t+1)} \tilde{B}H_\lambda \\ L_n &= H_\lambda^\top R H_x + (\tilde{B}H_\lambda)^\top V_{(t+1)} (\tilde{A} + \tilde{B}H_x). \end{aligned} \quad (9)$$

Lastly, we compute the control input for the special case where $\tau = 0$. The input $u[0]$ takes the form from Theorem 3, and we know the state at time $t = 0$ is zero. We have the control given by

$$\begin{aligned} u[0] &= H_\lambda \lambda^* + w \\ \lambda^* &= \operatorname{argmin}_{\lambda} (H_\lambda \lambda + w)^\top R (H_\lambda \lambda + w) \\ &\quad + \left[\begin{bmatrix} \vec{I} \\ \tilde{B}_0(H_\lambda \lambda + w) \end{bmatrix} \right]^\top V_{(1)} \left[\begin{bmatrix} \vec{I} \\ \tilde{B}_0(H_\lambda \lambda + w) \end{bmatrix} \right] \end{aligned} \quad (10)$$

The steps are enumerated in Algorithm 4.

Algorithm 4 DP with Quadratic Objective

Input: Per-step costs $g_\tau(\Phi_{xx}[\tau], \Phi_{xy}[\tau], \Phi_{ux}[\tau], \Phi_{uy}[\tau])$ for all $\tau = 0, \dots, T$ and the matrices A, B, C in (1); Q and R .

Output: $\Phi_{xx}[\tau], \Phi_{xy}[\tau], \Phi_{ux}[\tau], \Phi_{uy}[\tau]$ for all $\tau = 0, \dots, T$.

- 1: Derive h_τ from g_τ for all $\tau = 0, \dots, T$.
 - 2: Derive $\tilde{A}, \tilde{B}, \tilde{A}_{eq}$, and \tilde{B}_0 from A, B and C according to (1).
 - 3: $\Psi_x[T+1] = I$.
 - 4: $V_{T+1}(x[T+1]) = 0$.
 - 5: **for** $\tau = T, \dots, 1$ **do**
 - 6: Derive $\mathcal{A}_u[\tau]$ and $\Psi_x[\tau]$ by Theorem 2.
 - 7: Compute $K_\tau(x[\tau])$ by (9).
 - 8: Derive $V_\tau(x_\tau)$ by (8).
 - 9: **end for**
 - 10: Derive $\mathcal{A}_u[0]$ by Theorem 3.
 - 11: Compute $u[0]$ by (10).
 - 12: Set $\Phi_{uy}[0] = u[0]$ and $\Phi_{xx}[0] = \Phi_{xy}[0] = \Phi_{ux}[0] = 0$.
 - 13: Compute $x[1]$ by (4c).
 - 14: Perform line 14 to 18 in Algorithm 1.
-

V. EVALUATION

To evaluate the performance of our algorithm, we compare the time required to run our nominal algorithm and approximation algorithm with the solution given by CVX. We construct a set of stochastic chain matrices and time the computations for the \mathcal{H}_2 and quadratic objectives for the CVX algorithm, dynamic programming (Algorithm 3 and Algorithm 4), and their corresponding approximation algorithm (in the form of Algorithm 2). Additionally, we determine in which scenarios the approximation algorithm produces transfer functions that successfully attenuate disturbances. The data was generated on a desktop with an AMD Ryzen 7 3700X processor (16 logical cores) and 32 GB DDR4 memory; the CVX code was taken from SLSpy [14].

A. Evaluation Setup

The test system is a stochastic chain with state dimension N_x , input dimension N_u , and observation dimension N_y , which takes the form

$$A = \begin{bmatrix} 1-\alpha & \alpha & & & \\ \alpha & 1-2\alpha & \alpha & & \\ & \ddots & \ddots & \ddots & \\ & & \alpha & 1-2\alpha & \alpha \\ & & & \alpha & 1-\alpha \end{bmatrix}$$

$$B = \begin{bmatrix} I_{N_u} \\ 0 \end{bmatrix} \quad C = \begin{bmatrix} I_{N_y} & 0 \end{bmatrix}$$

where $\alpha \in (0, 1)$ and I_N is the identity matrix of size N . We set D to zero and do not use a constraint set. We construct the test cases to span the size ranges $N_x \in [5, 20]$ with $N_u = N_y = N_x$ and $T = 10$. Let T be the length of the finite impulse response (FIR) horizon; we run scenarios with

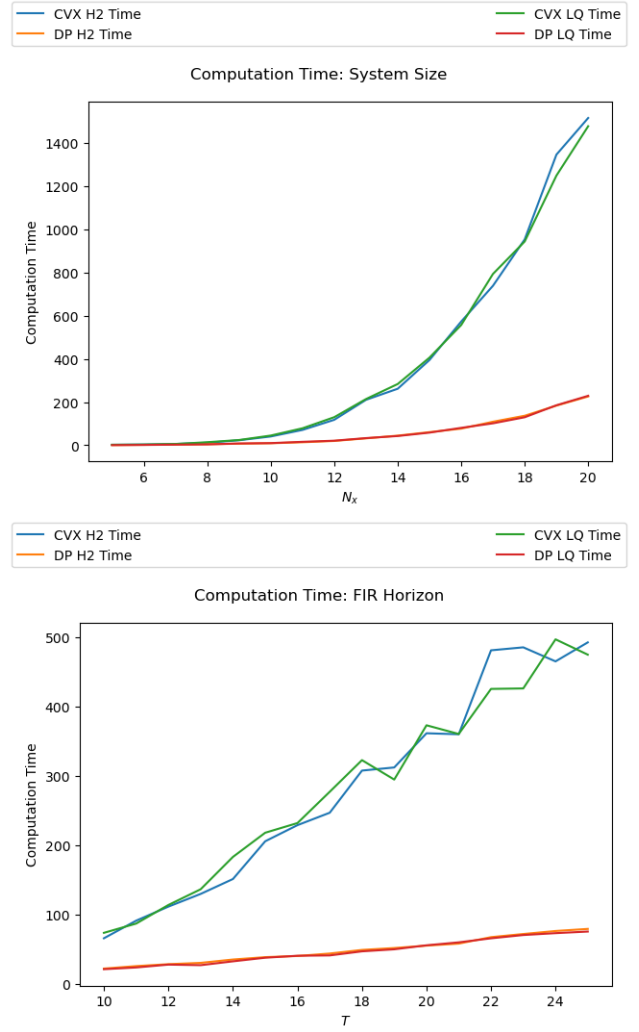


Fig. 1. The dynamic programming algorithms outperforms the CVX algorithms for both the \mathcal{H}_2 and quadratic objectives.

$T \in [10, 25]$ with $N_x = N_u = N_y = 10$. For both tests, we run 50 simulations per data point. The computing time is defined as the time required to compute Algorithm 3 or Algorithm 4, which includes constructing the reformulated matrices \tilde{A}, \tilde{B} and new cost function h_τ . Analogously, the computing time for CVX is the time required to synthesize the stabilizing controller under Algorithm 3 or Algorithm 4.

B. Computation Time and Scalability

We plot the computing time as a function of each problem dimension (N_x and T) for the \mathcal{H}_2 and quadratic objectives to compare the algorithms' scalability. Fig. 1 illustrates how the DP algorithm reduces the computation time compared with using CVX; for large values of N_x , DP is more than 5 times faster than CVX and for large T it is at least 6 times faster. The greatest improvement is computed as over 7 times faster for N_x for the quadratic objective. We also observe that the time increases more slowly with increasing system dimensions compared with CVX for larger system dimensions, showing the scalability of our methods.

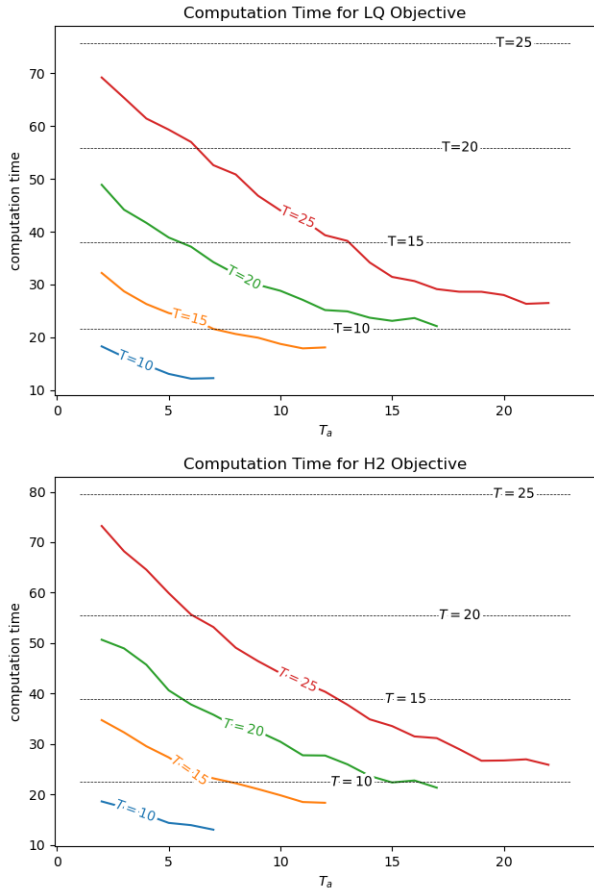


Fig. 2. As the number of steps at which H_X and H_Λ are not recomputed increases, the time needed to compute the solution decreases. The dashed lines show the average computation time for the full SLS DP method.

C. Convergence of Approximation Algorithm

The approximation algorithm partially removes the constraint requiring that the transfer functions at time $T + 1$ are zero, which removes the guarantee that disturbances will be killed off in exchange for skipping expensive nullspace computations. We test scenarios with varying values of the allowance T_a , which is the number of nullspace computations skipped, and record whether the transfer functions properly terminate disturbances within the finite impulse response time. In Fig. 2, we see that avoiding computations of \mathcal{A}_u for every time step in the FIR horizon significantly improves the overall computation time relative to the plain DP algorithm; run time decrease by 42% to 68% for the largest allowances, and we see the largest percentage improvements for systems with the largest FIR horizon. For all $T \in [10, 25]$, for all $T - T_a \leq 3$, and for each of the 50 test simulations, we verified that the solution was in fact optimal.

VI. CONCLUSION

We derived DP algorithms to solve output-feedback SLS problems by reformulating the optimization constraints as a linear control problem, using two stages of DP to enforce boundary conditions and an interior condition. We illustrated

specific examples of our DP algorithm on the \mathcal{H}_2 and quadratic objectives, along with computation time results of each. The simulation results show that DP, including the approximation DP, outperforms the traditional CVX solver. Future work includes deriving either deterministic or probabilistic guarantees for when the approximation algorithm converges, given broader classes of systems beyond stochastic chains. Additionally, we want to investigate the robustness of this method to model uncertainty.

REFERENCES

- [1] J. C. Doyle, B. A. Francis, and A. R. Tannenbaum, *Feedback Control Theory*. Courier Corporation, 1992.
- [2] K. Zhou, J. C. Doyle, K. Glover *et al.*, *Robust and Optimal Control*. Prentice hall New Jersey, 1996.
- [3] J. Anderson, J. C. Doyle, S. H. Low, and N. Matni, "System level synthesis," *Annual Reviews in Control*, vol. 59, no. 12, pp. 3238–3251, 2019.
- [4] Y.-S. Wang, N. Matni, and J. C. Doyle, "A system level approach to controller synthesis," *IEEE Trans. Autom. Control*, vol. 34, no. 8, pp. 982–987, 2019.
- [5] L. Furieri, Y. Zheng, A. Papachristodoulou, and M. Kamgarpour, "An input-output parametrization of stabilizing controllers: Amidst Youla and system level synthesis," *IEEE Control Systems Letters*, vol. 3, no. 4, pp. 1014–1019, 2019.
- [6] Ş. Sabão and N. C. Martins, "Youla-like parametrizations subject to QI subspace constraints," *IEEE Trans. Autom. Control*, vol. 59, no. 6, pp. 1411–1422, 2014.
- [7] D. C. Youla, H. A. Jabr, and J. J. Bongiorno Jr., "Modern Wiener-Hopf design of optimal controllers – part II: The multivariable case," *IEEE Trans. Autom. Control*, vol. 21, no. 3, pp. 319–338, 1976.
- [8] Y.-S. Wang, N. Matni, and J. C. Doyle, "Separable and localized system-level synthesis for large-scale systems," *IEEE Trans. Autom. Control*, vol. 63, no. 12, pp. 4234–4249, 2018.
- [9] J. Anderson and N. Matni, "Structured state space realizations for SLS distributed controllers," in *Proc. Allerton*, 2017, pp. 982–987.
- [10] N. Matni, Y.-S. Wang, and J. Anderson, "Scalable system level synthesis for virtually localizable systems," in *Proc. IEEE CDC*. IEEE, 2017, pp. 3473–3480.
- [11] C. Amo Alonso and N. Matni, "Distributed and localized closed loop model predictive control via system level synthesis," in *Proc. IEEE CDC*. IEEE, 2020, pp. 5598–5605.
- [12] C. Amo Alonso and S.-H. Tseng, "Effective GPU parallelization of distributed and localized model predictive control."
- [13] S.-H. Tseng, C. Amo Alonso, and S. Han, "System level synthesis via dynamic programming," in *Proc. IEEE CDC*, Dec. 2020.
- [14] SLSpy. [Online]. Available: <https://github.com/shih-hao-tseng/SLSpy>
- [15] S.-H. Tseng, "Realization, internal stability, and controller synthesis," in *Proc. IEEE ACC*, May 2021.